

# **Evaluating the Effects of Underground Nuclear Testing Below the Water Table on Groundwater and Radionuclide Migration in the Tuff Pile 1 Region of Yucca Flat: Numerical Simulations**

(FY 99 Report)

Kenneth Wohletz, Andrew Wolfsberg, Alyssa Olson, and Carl Gable

## **ABSTRACT**

Initial scoping numerical simulations, using FEHM, evaluate perturbed groundwater behavior associated with underground nuclear tests in the Tuff Pile 1 area of Yucca Flat. Because many of these tests were conducted below the water table, we direct our simulations to a preliminary study of the sensitivity of the saturated pressure response to an instantaneous pressurization event caused by a nuclear test when different permeability and porosity configurations are considered. Geologic and hydrostratigraphic data were digitized for the area to create a 3-D simulation mesh. We modeled underground nuclear tests with sufficient numerical resolution to resolve spherical regions within the mesh with radii scaled to reported yields and surrounding disturbed zone extending to 2 cavity radii. Ranges of appropriate rock permeability and porosity values allow a number of different model cases to be studied. Of these cases, ones that considered the disturbed zone to be contained within low permeability rocks may best model observations of water mounding in the area. For these cases, hydraulic head increases in rocks up to 4 cavity radii away from tests for up to 100 years after the test and require over 1000 years to return to a pretest state. For deep tests, this pressurization extends into the regional aquifer, indicating a possibility that fluids originating near the boundary of the disturbed zone will eventually move into the regional aquifer. In cases where the disturbed zone extends into higher permeability rocks, there is a rapid decay of overpressure. Future work requires detailed hydrologic analysis of shot cavities and disturbed zones, consideration of unsaturated rocks, solute transport modeling, and testing with observed water rise heights and rates.

## **INTRODUCTION**

Numerous observations of anomalously high water levels (water mounding) in drill holes, sited in the vicinity of Tuff Pile 1 (Areas 1, 3, 4, and 7 of the Nevada Test Site), are coupled to measurements of radionuclide contamination in groundwater sampled from areas nearby. An evaluation of hydrogeologic studies in this area suggests that underground nuclear testing has disturbed the natural hydrologic environment by rock deformation that exists in regions surrounding test working points (Wohletz and Hawkins, 1998). The rock deformation that accompanies underground nuclear testing includes regions where pore space has been greatly reduced, making previously partly saturated rocks fully saturated and/or displacing pore water above the area's static water level. This deformation combined with the creation of fractures extending radially from working points likely contributes to migration of contaminants from the cavity and chimney regions of tests. The degree to which contaminant migration may have affected the regional aquifer, existing in carbonate basement rocks several hundred meters below the working points is not known.

In this report we describe initial numerical simulations aimed to test the hypothesis that underground testing can pressurize aquifer rocks, produce anomalous hydraulic heads, and provide predictions as to whether the aquifer pressurization may have driven contaminants downward to the regional aquifer. The simulations employ the FEHM code (Zyvoloski et al., 1992), which has shown considerable applicability to similar kinds of problems for other NTS-UGTA studies, for the Yucca Mountain project, and for environmental restoration (ER) studies at Los Alamos and in Northern New Mexico.

Several important tasks had to be completed in order to provide suitable boundary and initial conditions for FEHM. For initial and boundary conditions, we used data in existing data bases, provided by the USGS and Bechtel Nevada, as well as LANL underground testing data bases. All of these sources are in the open literature. Under the section titled Simulation Technique, we describe how stratigraphic information was digitized in order to produce the mesh variables required for the simulations, how we assigned physical and hydrological properties to these rocks, and the location, size, and typical character of cavities and deformed rock surrounding the 26 (18 below the water table) historical tests in this area.

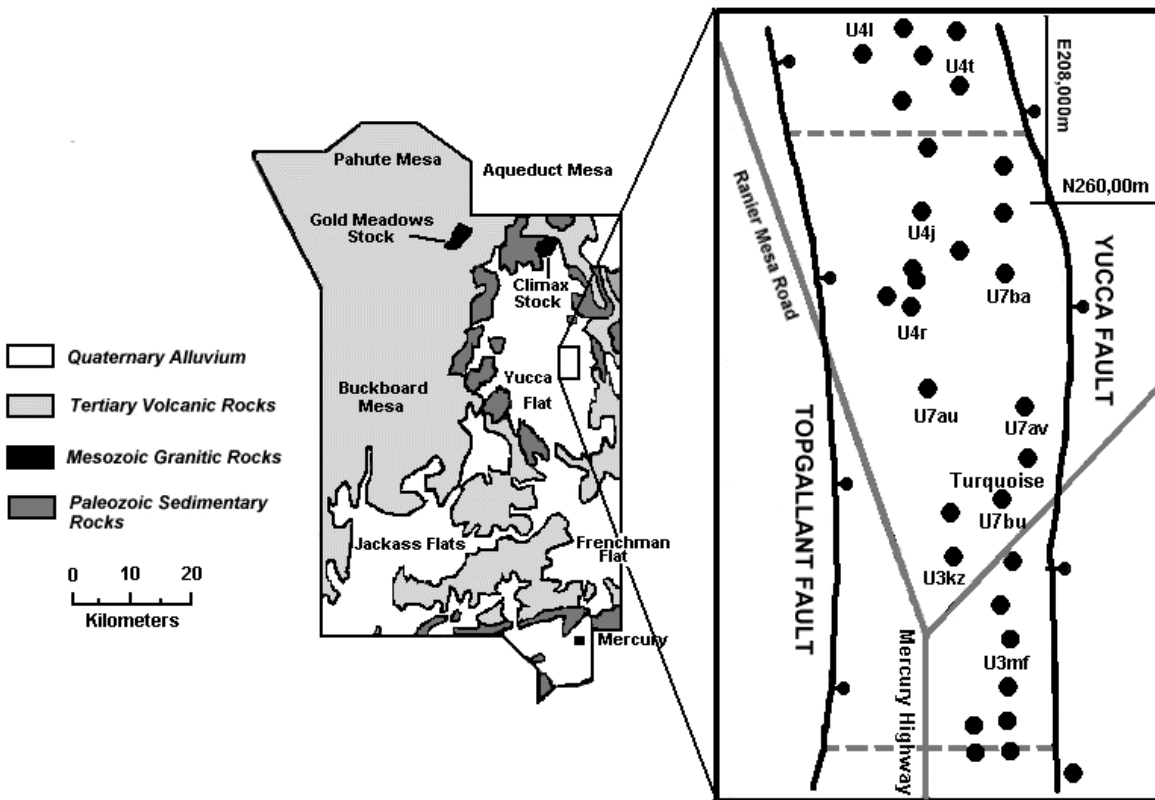


Figure 1. Tuff Pile 1 location map, showing locations of underground tests.

## SIMULATION TECHNIQUE

In order to apply FEHM to simulations of a disturbed hydrologic regime within the Tuff Pile, we follow a step-by-step procedure, embodied in the following modeling framework. This framework involves a process of:

1. Geologic interpretation
2. Identification of the tops of hydrostratigraphic surfaces (HSU)
3. Development of three-dimensional geologic model
4. Numerical discretization of the geologic model into a finite-element grid for flow simulations
5. Identification of spatial properties (permeability and porosity) at nodes in the grid
6. Identification of boundary conditions
7. Simulation of flow on the undisturbed system
8. Simulation of flow on a system with perturbed pressure and properties
9. Evaluation and analysis of simulated responses.
10. Preliminary transport calculations

With the established modeling framework, we illustrate a number of test cases that include a partial sensitivity analysis focussing on the importance of permeability within host rocks and the disturbed zone surrounding test cavities. Summarizing these results, we then describe the affect of calculated hydraulic head on fluid transport.

### Modeling Framework

The modeling framework includes the hydrogeological model, grid generation properties, boundary and initial conditions, modeling the disturbed state, model response observations, and physical and hydrologic properties.

**Hydrogeological Model.** The Tuff Pile encompasses about 8 km<sup>2</sup>, including parts of Areas 1, 3, 4, and 7 north of Nevada state coordinate N256,000 m. It is situated between the Yucca fault to the east and the Topgallant fault to the west (Fig. 1), both of which dip towards the east. The geology and geophysics of this area are now so well known and predictable that most characteristics required for test containment evaluation no longer need to be measured but can be predicted by location with only several percent of error (App and Marusak, 1997). This predictability lends considerable confidence to our effort in characterizing the hydrogeology of the area, a characterization that depends largely upon the stratigraphic sequence.

A 2000-foot sequence of Tertiary volcanic rocks, mostly tuffs, overlies basement rocks consisting mostly of Paleozoic carbonates, which contain the regional aquifer. The Tertiary sequence shown in Figure 3, which includes example cross sections through U7aq-U7au (Sandreef-Rummy) and U3kz (E-W; Aleman). These cross sections show that the Tertiary strata are mostly flat-lying from south to north displaying a uniform westerly dip from west to east. These cross sections identify tuffs below the Rainier Mesa Tuff as Paintbrush Tuff, but more

recent work (e.g., Drellack, 1994) indicate that the Rainier Mesa Tuff pinches out south of the Tuff Pile 1 area.

The simplified hydrogeology of the area consists of basically five HSUs from top to bottom: (1) the alluvial aquifer; (2) the welded tuff aquifer (Ammonia Tanks and Rainier Mesa tuffs); (3) the vitric tuff aquifer (pre-Rainier post-Wahmonie bedded tuffs); (4) the tuff confining unit; and the (5) the lower carbonate regional aquifer (pre-Tertiary carbonate rocks). The hydrogeologic character of these HSUs is shown in Table 1. Rocks below the welded tuff (Rainier Mesa Tuff) are characteristically zeolitized. The top of zeolitization extends up into the welded tuff HSU in places. The static water level generally exists at the base of the welded tuff and includes the welded-tuff aquifer and vitric-tuff aquifer.

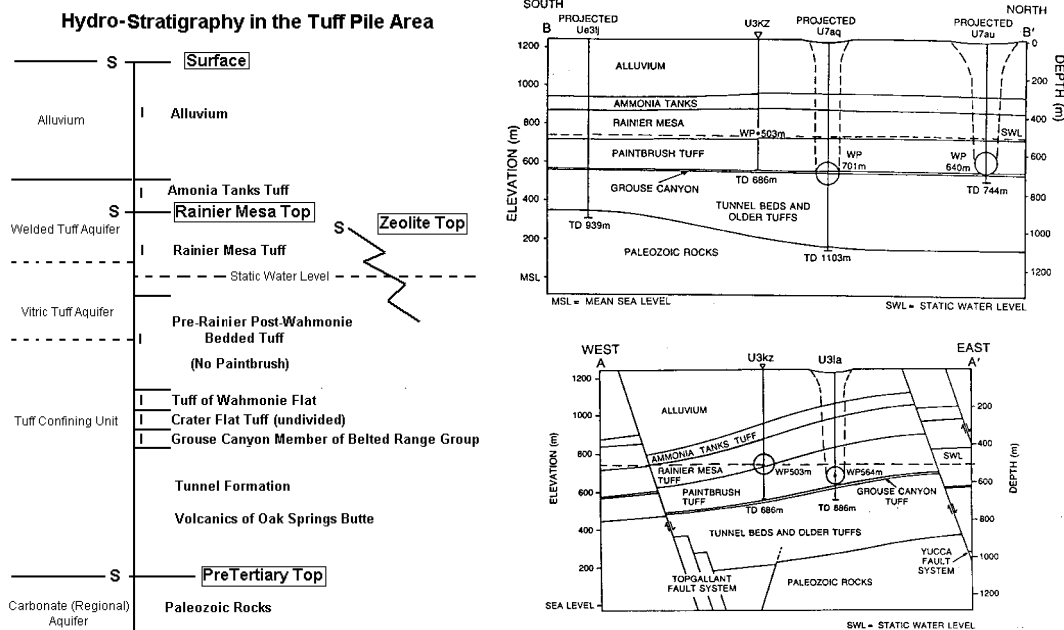


**Figure 3.** Hydrostratigraphic units and example cross sections for the Tuff Pile 1 Areas of Yucca Flats. “S” indicates contacts for which structural contours have been measured and digitized, “I” indicates units whose isopach thickness have been measured and digitized. The boundaries between the welded tuff, vitric tuff, and tuff confining units are at variable depths and largely depend upon the depth at which zeolitization occurs. The cross sections are adapted from Hawkins and Cavazos (1987).

Most structural and isopach contour data has been measured and plotted on maps by Raytheon Services Nevada (now Bechtel Nevada) and documented in technical memoranda by S. L. Drellack over a period from 1988 to 1995. Through personal communications with Drellack, we obtained the most recent revisions to this data set.

In order to use these structural and isopach data, we digitized the contours from the Nevada State Plane and convert them to UTM. This task was accomplished by a program we developed called DigiMap. Figure 4 is an example digitization for the pre-Tertiary surface. Digitized points were chosen along mapped contours at average intervals of about 100 m and <50 for areas where detail was greatest. DigiMap allows adding and subtracting isopach contours in order to produce

structural contours for intervals that only have isopach data. In addition the surface topography (USGS 1968 1:24,000 series; prior to underground nuclear testing in this area) and static water level elevations (Hoover and Trudeau, 1987) were also digitized. For these modeling simulations, we focus attention on the saturated zone such that the water table surface truncates the geologic model, thus defining the top of the simulation domain.

**Table 1. Hydrogeological Characteristics of the Tuff Pile 1 Area**

<i>Hydrostratigraphic Unit</i>	<i>Characteristics</i>
1. Alluvial Aquifer	Generally unsaturated
2. Welded Tuff Aquifer	Saturated only in western areas near the Topgallant fault system. Porosity decreases but (fracture) permeability increases with increasing welding (dense welding only in middle part of the Rainier Mesa Tuff).
3. Vitric Tuff Aquifer	Saturated in western areas. Contains significant porosity (20 – 40%), but has insignificant fracture permeability
4. Tuff Confining Unit	Generally saturated, zeolitized bedded tuffs of very low porosity and permeability. Major confining unit.
5. Carbonate Aquifer	Important regional aquifer with thickness up to 4400 m. Permeability directly dependent upon fracture and fault frequency

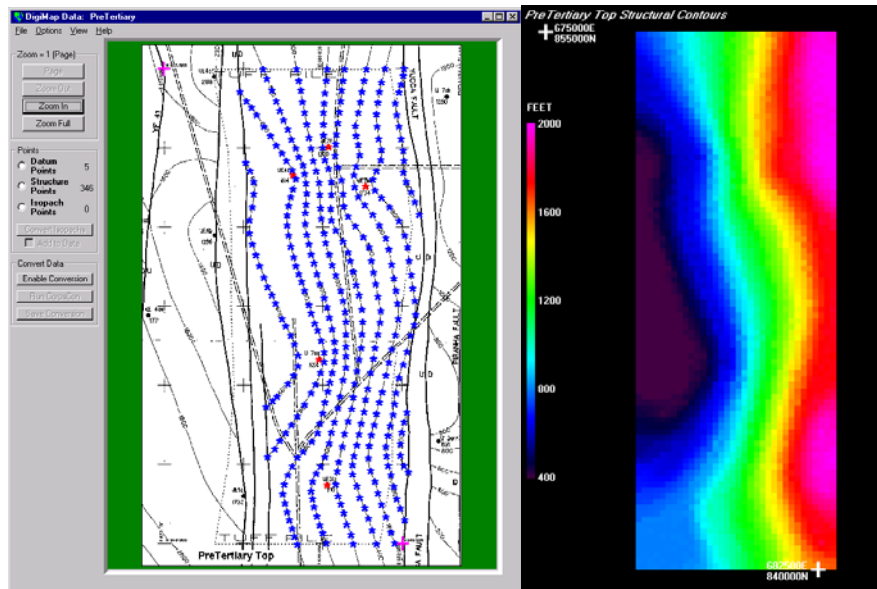


**Figure 4.** Contours defining the top of the pre-Tertiary unit and the resulting digitized surface for input to the three-dimensional model.

These digitized surfaces of the HSU tops were then read into the Los Alamos Grid Generation Toolbox software (LaGriT). Prior to generating the actual computational grid, LaGriT fills in the volumes between surfaces, rendering a three-dimensional geologic model of the domain. The results can be visualized with virtually any three-dimensional graphics package (Figure 5). These layers are used to populate the computational grid with properties unique to each unit. Not shown in the Figure 5 is the surface below which zeolitization is prominent and above which little alteration is expected. However, that surface is also used later by LaGriT to specify material properties in addition to those unique to each unit.

**Grid Generation and Properties.** Utilizing the surfaces defining the tops of HSUs and the water table, LaGriT automatically generates a finite element grid capturing accurately the structure of the HSUs and the contacts between them. This leads to very high resolution in the thin units such as the Grouse Canyon and Wahmonie tuffs and relatively coarse resolution in such thick units as the pre-Tertiary unit. During the grid generation process, additional resolution can be prescribed by the user to guarantee a minimum resolution in the resulting finite-element grid. Such control was used here to insure appropriate resolution in the thicker units and to insure accurate spherical resolution up to 2 cavity radii about each test.

After generating the finite-element mesh, LaGriT identifies each node in the domain by the material unit it is contained within. LaGriT was also used in this study to provide information about each node's proximity to the 26 working points of the underground nuclear tests conducted within the model domain. Appendix A provides the locations of the tests, the yield ranges, the radius computed from the maximum announced yield and other information. In this model, each test is identified along with the nodes surrounding the working point at specified distances. The conceptual models tested in this study examine the effects resulting from material alteration and pressure anomalies in the zones defined by 1, 1.3, and 2 cavity radii about each test. Figure 6 shows the nodes defined within 1.3 and 2 cavity radii of the shots. Here the cavity radius for each shot is assumed to be the maximum estimated radius computed from the maximum of the range of reported yields. Clearly, as larger radial distances are considered, the volume of material identified with each shot increases. Also, as some nodes could actually be *owned* by multiple shots, they are identified chronologically as the shots were conducted. Thus, if a node were within  $2r_a$  of shot  $a$ , but then another test, shot  $b$ , was conducted later and its  $2r_b$  domain encompassed that node, then the node is assigned to test  $b$  for the  $2r$  identification. The identification of nodes by radial distances from shots and by HSU will be discussed more in the simulations sections.

**Boundary conditions.** As described above the water table elevation map from Hoover and Trudeau (1987) was digitized to establish the contour map shown in Figure 7. In addition to providing the upper boundary for the model, the values of hydraulic head at the edges of this map were used to generate a steady state, pre-testing flow solution.

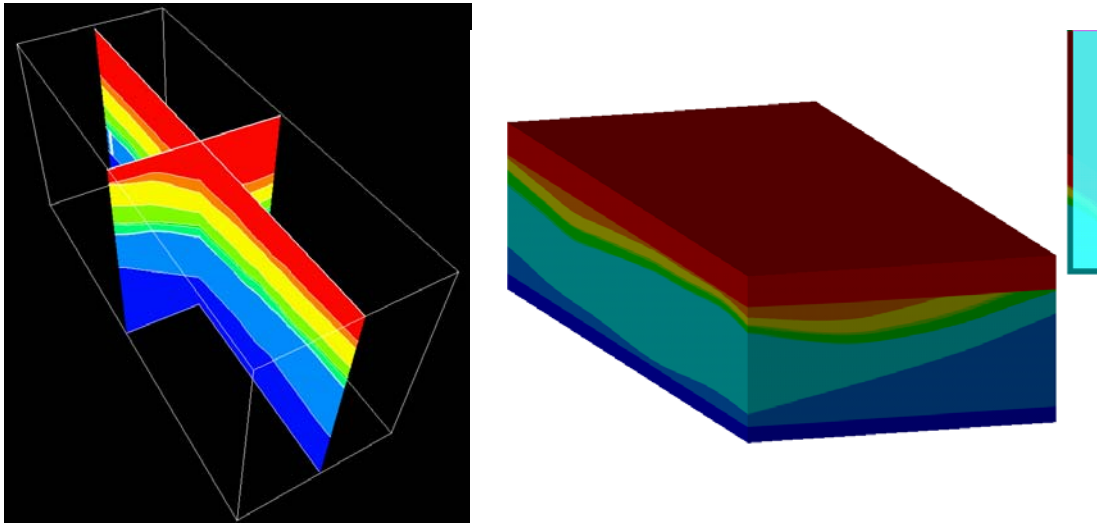


**Figure 5.** Cross section (NE to SW) and block (SW-NE) views of model grid, each color represents a different tuff layer. Tuffs are identified top to bottom in Figure 3.

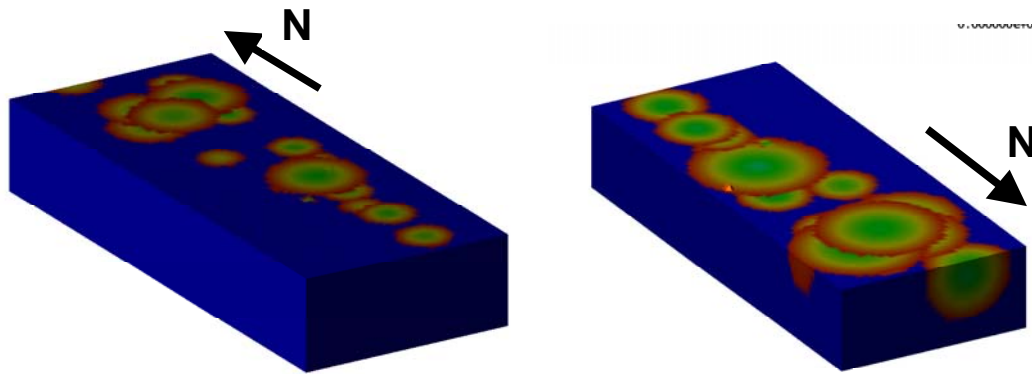


**Figure 6.** Visual images colored by radial property showing the nodes associated with the 1.3 cavity radius on the left and the 2.0 cavity radius on the right.

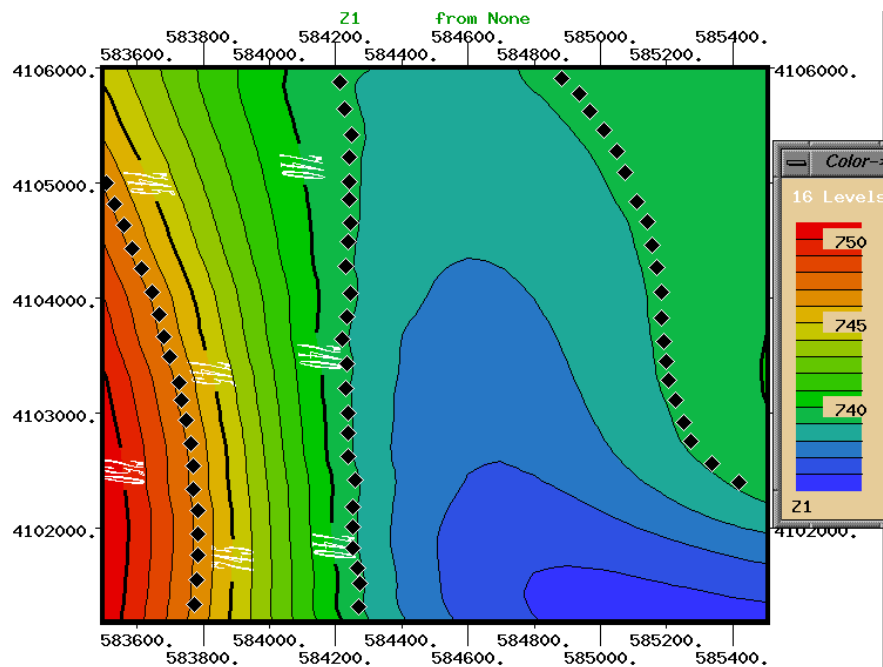


**Figure 7.** Water table elevation map digitized from the map published by Hoover and Trudeau (1987). Model boundary heads are set by the values in this map.

***Initial conditions: Steady state flow prior to testing.*** Using the hydraulic head values along the boundary of the model domain, we calculated a steady state flow solution for each different set of hydrologic parameters (permeability and porosity) considered for pre-testing conditions. These different models examine various parameterizations of the different tuff units, the zeolitized and non-zeolitized portion of the domain, and the pre-Tertiary rocks. For each case the model was run to a steady state solution, providing an initial condition for the simulated perturbations in pressure and properties resulting from underground nuclear testing.

***Modeling the Disturbed State.*** Due to the paucity of data, there are no measurements with which to specify changes in hydrologic parameters in the vicinity of a test, after the explosion. Therefore, several hypotheses describing possible property changes that could lead to the observed water mounding phenomenon are considered in this preliminary sensitivity analysis. The conceptual models examined here are derived from Lacznik and others (1996), which summarizes what is known about the effects of nuclear testing on ground water flow and hydrologic properties. According to the summary, the area within 1.3 cavity radii of a working point is intensely pulverized and the area between 1.3 and 2 cavity radii is tightly compacted by the compressional shock wave that passes through the media. Our simulations, then, are based on the hypothesis that within the compacted region, pressure increases substantially due to a) porosity decrease resulting from compaction and b) the possible additional pressurization due to

water and water vapor being forced out of the cavity during and soon after the explosion. Based on this conceptual model, elevated pressure is prescribed in the zone between  $1.3r$  and  $2r$  for each test in the model domain and simulated responses both in and away from the cavity are monitored. It is currently not known how high the hydraulic pressure in the disturbed zone rises just after a shot. Such a pressure could be estimated by considering the volume of fluid in the cavity and the reduction of volume due to compaction in the disturbed zone. However, since the primary purpose of this modeling exercise is to test the functionality of the model and, in a sense, to prove the concept and approach, a somewhat arbitrary value of 2000 m is specified in the disturbed zone for each test. This value is sufficiently higher than any of the pre-testing heads in the domain (maximum 760 m), so it provides a perturbation from which to monitor the response in the domain over time. In all of the simulations, the permeability of the cavity is increased after the testing. The permeability and porosity of the disturbed zone are treated as an uncertain variable and the sensitivity to those parameters is examined with multiple different simulations. It must also be noted here that all of the tests are assumed to have occurred at the same time in this initial set of simulations. Clearly, the next iteration will consider the 20 years over which the testing occurred when introducing the pressure and property changes to the system.

***Model response observations.*** An array of observation points was selected to look at the time history of hydraulic head after testing at various places in the grid. These observation points are shown on a plan view plot of the model domain in Figure 8. The figure shows only lines 2 and 3 because line 1 extends downward from the WP toward the carbonate aquifer. All three of the lines originate at the same shot, the Turquoise event (U7bu), and the observation points on lines 2 and 3 are at approximately the same elevation as the working point for Turquoise. Most of the nodes on lines 2 and 3 are in non-zeolitized areas excepts for those nodes closest to the working points. The positions in space of the nodes, the geologic units, the distance from the working point (WP) and the distance as a function of the cavity radius are all given in Table 2. These observation points were used to document how the increased pressure in the disturbed zone dissipated into the surrounding rock under varying permeability and porosity conditions. Also shown in Table 2 are the line numbers for each observation point.

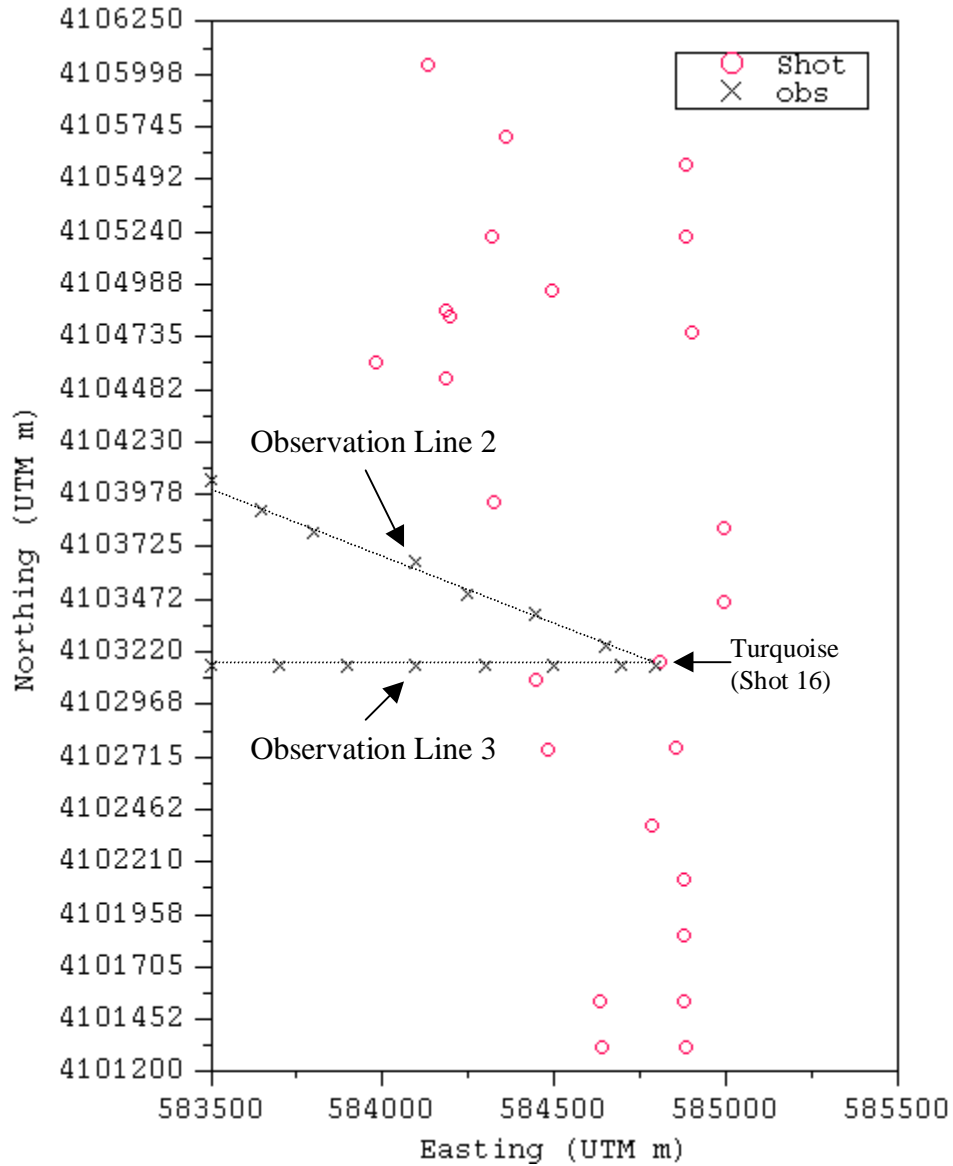


**Figure 8.** Plan view plot of Yucca Flat showing the shot locations and the locations of lines 2 and 3. Line 1 extends downward from the Turquoise shot (Shot 16) toward and into the carbonate aquifer

Table2. Observation Point Locations in Model Domain

Line NO.	Obs. Point Node in Grid	Geologic Unit , Alteration and Relation to Shot Modification	Easting (m)	Northing (m)	Elev (m)	Distance from the WP	*r
1	18433	Carbonate Aquifer	584800	4103150	7	706.47	2.1
1	26387	Carbonate Aquifer, Disturbed Zone	584800	4103150	101.18	612.36	1.82
1	34341	Carbonate Aquifer, Disturbed Zone	584800	4103150	200.35	513.29	1.53
1	42258	Carbonate Aquifer, Cavity	584800	4103150	299.53	414.26	1.23
1	58161	Zeolitized Tunnel Formation, Cavity	584800	4103150	407.24	306.83	0.91
1	66115	Zeolitized Tunnel Formation, Cavity	584800	4103150	523.48	191.25	0.57
1	74064	Zeolitized Tunnel Formation, Cavity	584800	4103150	633.27	83.75	0.25
1,2,3	90374	Zeolitized Crater Flat Tuff, Cavity	584800	4103150	721.40	26.97	0.08
2	102362	Zeolitized Pre-Rainer, Post-Wahmonie Tuff, Cavity	584700	4103150	711.26	111.62	0.33
2	106516	Pre-Rainer, Post-Wahmonie Tuff, Cavity	584500	4103150	730.38	310.42	0.92
2	108957	Rainer Mesa Tuff, Cavity	584300	4103150	711.61	509.57	1.52
2	111644	Rainer Mesa Tuff	584100	4103150	712.01	709.41	2.11
2	111348	Rainer Mesa Tuff	583900	4103150	708.31	909.33	2.71
2	109579	Rainer Mesa Tuff	583700	4103150	715.27	1109.26	3.30
3	104491	Zeolitized Pre-Rainer, Post-Wahmonie Tuff, Cavity	584650	4103250	716.87	176.27	0.52
3	106454	Pre-Rainer, Post-Wahmonie Tuff, Cavity	584450	4103400	732.75	424.67	1.26
3	110414	Rainer Mesa Tuff, Disturbed Zone	584250	4103500	713.34	647.11	1.93
3	111654	Rainer Mesa Tuff	584100	4103650	711.93	583.97	2.54
3	111201	Rainer Mesa Tuff	583800	4103800	713.18	1189.42	3.53
3	110947	Rainer Mesa Tuff	583650	4103900	717.59	1367.62	4.07

**Assigning Physical and Hydrological Properties to these Rocks.** Due to the minimal available hydrological data for Yucca Flat rock properties, ranges from the known published data and estimates were used in these scoping calculations. The permeability data used in this study to assign rock properties is presented in Table 3. The rock density (bulk and grain) and porosities used for each formation are tabulated by App and Marusak (1997) for both saturated and unsaturated zones and are essentially the same for both the zeolitized and non-zeolitized units. Table 4 gives the saturated porosities and the respective formation as applied to the numerical simulations.

Due to the lack post-test hydrologic data, model properties for the cavity and disturbed zone are uncertain. They are treated here with a partial sensitivity analysis. The region out to  $1.3r$  for each test is assumed to have higher permeability than the pretest conditions due to rubblization and chimney collapse. The porosity in that region is also assumed to be at least as high as the pre-test porosity. The permeability in the disturbed zone ( $1.3r$  to  $2r$ ) is varied. It is set either equal to the pretest permeability of the various HSUs into which the disturbed zone for each test extends and then, it is set even lower to represent additional compaction. The porosities are set similarly, with a reduction by a factor of ten when compaction is considered.

**Table 3. Permeability Ranges for Specific Units**

Source for permeabilities	Welded Tuff	Zeolitized Welded Tuff	Carbonate Aquifer	Post-shot Cavity	Disturbed Zone around the Post-shot Cavity
Winnograd and Others (1975)	$4.7 \times 10^{-12}$ to $6.0 \times 10^{-12}$ m <sup>2</sup> (n=2)	$3.24 \times 10^{-15}$ to $2.7 \times 10^{-18}$ m <sup>2</sup>	$6.0 \times 10^{-13}$ m <sup>2</sup> (geometric mean)	N/A	N/A
Flint(1998)	N/A	$1.15 \times 10^{-14}$ to $1.15 \times 10^{-19}$ m <sup>2</sup>	N/A	N/A	N/A
Estimated range for this work	$1 \times 10^{-12}$ to $1 \times 10^{-15}$ m <sup>2</sup>	N/A	$1 \times 10^{-13}$ to $1 \times 10^{-14}$ m <sup>2</sup>	$1 \times 10^{-13}$ m <sup>2</sup>	$1 \times 10^{-19}$ to $1 \times 10^{-20}$ m <sup>2</sup>

**Table 4. Rock Porosities in the Tuff Pile**

Formation	Porosity
Rainier Mesa Tuff	0.460
Pre-Rainer, Post –Wahmonie Bedded Tuff	0.400
Wahmonie Flat Tuff	0.400
Crater Flat Tuff	0.400
Grouse Canyon	0.411
Tunnel Formation	0.354
Pre-Tertiary Carbonate Aquifer	0.35
Cavity porosity	0.4
Disturbed zone around cavity (estimated)	0.04

## SIMULATION RESULTS

We conducted a number of simulations that explore the effects of porosity and permeability upon hydraulic head dissipation. The simulations that best illustrate results of this study can be grouped into four test cases. Results are shown as 2- and 3-D plots of head response over the Tuff Pile 1 domain and by head response at specific nodes as a function of time after the underground nuclear tests caused pressurization of the saturated zone (welded tuff and vitric tuff aquifers and the tuff confining unit). Analysis of these test cases allows us to make some preliminary interpretations described in the summary of test results. Finally we describe the results of simple fluid transport simulations for one of the test cases.

### Test Cases

The test cases described in this section represent the systematic evaluation of various property effects on the dissipation of the post-test hydraulic head perturbations specified in the disturbed zone. The test cases start with a simple base case and move toward greater complexity, incorporating changes in permeability and porosity. In each case, the pretest steady state flow field is first calculated for each change in material properties. Then, a 2000 m head perturbation is applied to all nodes in the disturbed zone of the tests below the water table. Although data limited and non-exhaustive, this study highlights important issues in understanding hydrologic controls on pressure dissipation processes and the water mounding observations in Yucca Flat.

**Case 1: Base Case—Uniform Low Permeability.** The base-case model was designed to investigate what undisturbed permeabilities could hinder the dissipation of pressure in less than 30 years. The lowest estimated permeability in the region,  $1 \times 10^{-19} \text{ m}^2$  taken from Table 3, and a porosity of 0.4 were applied uniformly over the entire domain. In the disturbed zone, the porosity was reduced from 0.4 to 0.04. The purpose of this case was to establish the response to the simplest field condition possible and to evaluate the ability of the low permeability tuffs to sustain a pressure pulse over large periods of time. Figures 9 and 10 show the head response in domain for this case over the first 100 years. Clearly, for the conditions specified here, a head mound persists over much of the domain during the first 100 years after testing.

Figure 11 and Figure 12 show the head response at the observation points during the post-test simulation. The hydraulic head at the observation points outside of the disturbed zone go up almost immediately and continue to increase until after 100 years at which time the head starts to decrease. Even after 1000 years, the levels at the observation points have not returned to the steady state, pre-testing condition. Since this case was conducted in a homogeneous medium the hydraulic head dissipates uniformly at any given distance from the working point, this is evident in the time history for the observation points at  $2.54r$  in Figure 11 and at  $2.1r$  in Figure 12. At 100 years in the simulation, a considerable increase in hydraulic head is visible at a distance of 3.53 cavity radii (or 1.1 kilometers from the working point) as shown in Figure 11. This case clearly shows that if a shot increases the hydraulic head around the cavity then low permeability tuffs and a reduction in porosity around the cavity are sufficient to create and maintain a water-mounding type phenomenon for a considerable length of time.

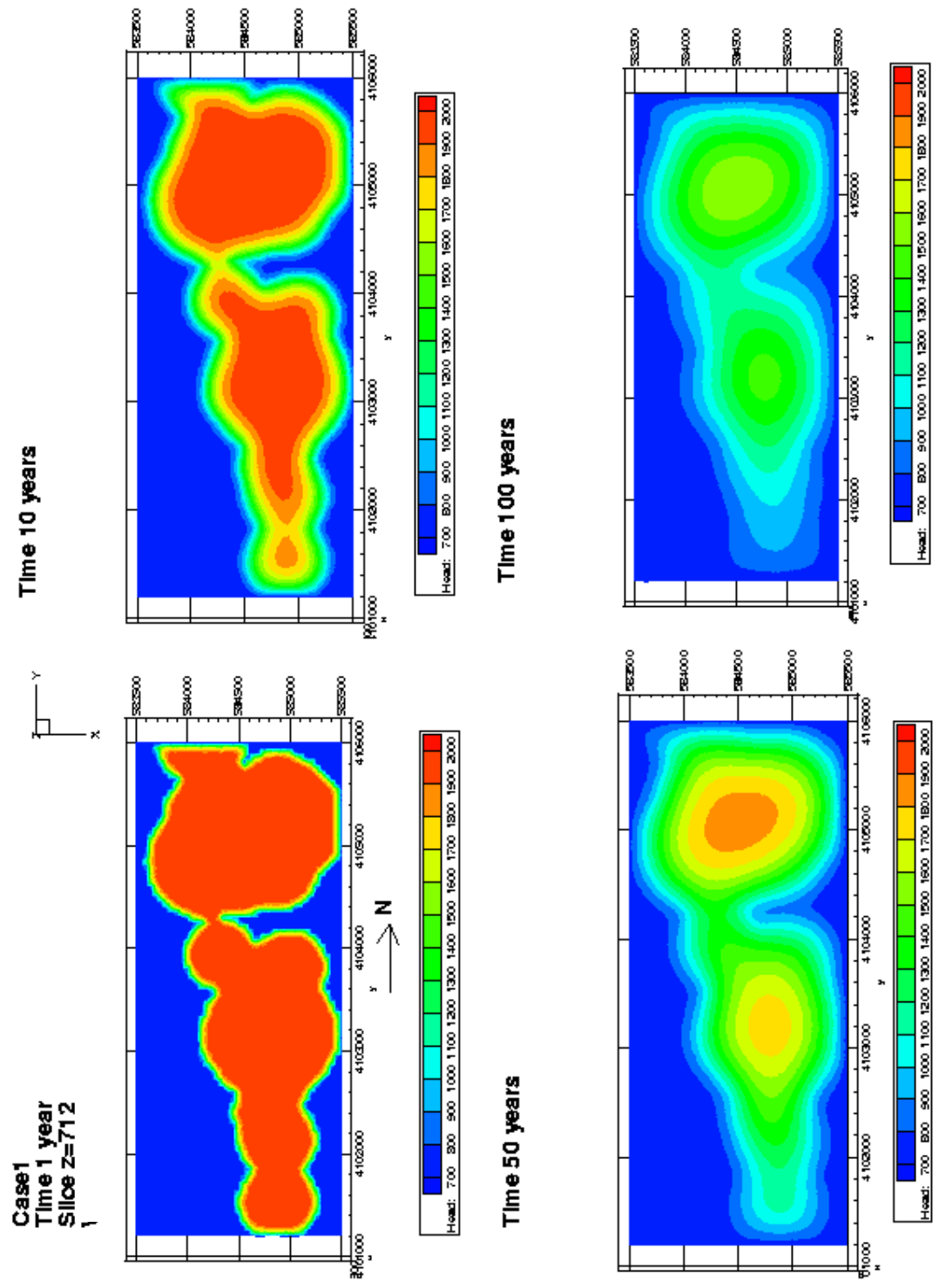
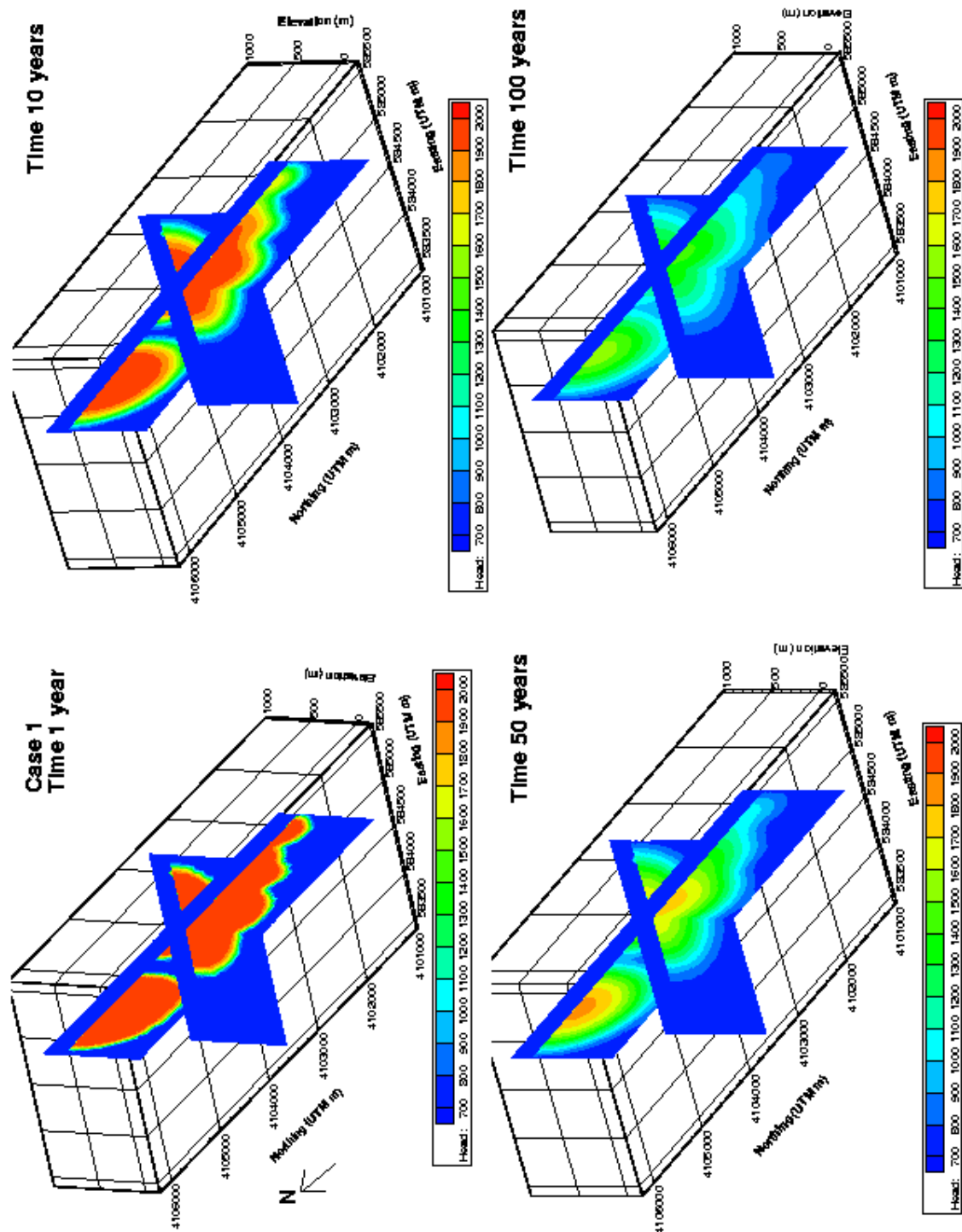
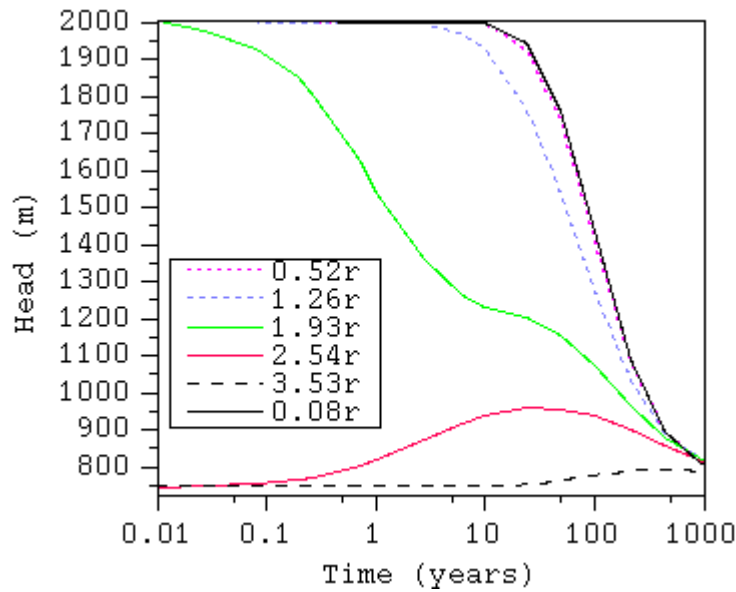


Figure 9. Simulated head response in domain over 100 years at elevation of Shot #16 working point (712m).



**Figure 10.** Head Responses throughout the domain over first 100 years for Case 1 conditions shown with vertical slices.



**Figure 11.** Simulated head responses on observation line 3 for Case 1. Plot shows decline in head over time within the disturbed zone and propagation of head pulse through points outside of the disturbed zone. Heads have not returned to pretest conditions outside of disturbed zone, even at 1000 years.

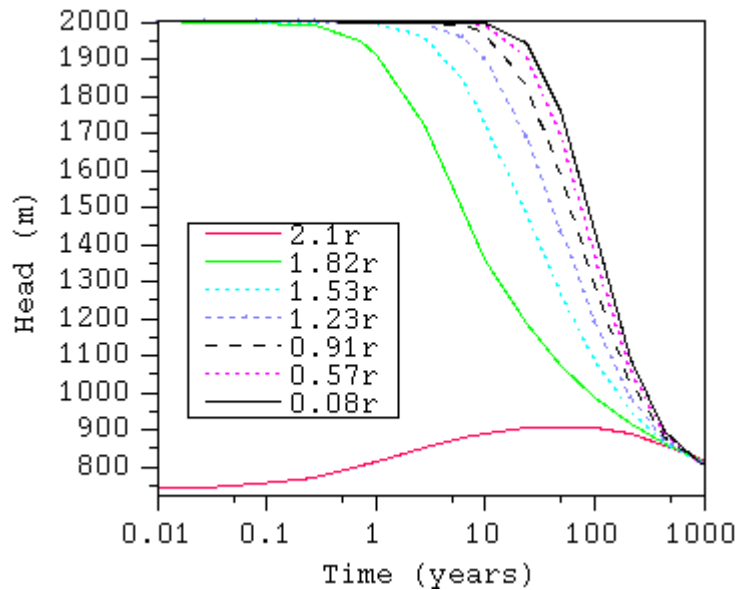


**Figure 12.** Simulated head responses on observation line 1 (downward from working point) for Case 1. Plot shows the gradual decline in hydraulic head inside the disturbed zone and the propagation of the head pulse through the observation point outside of the disturbed zone. Heads have not returned to pretest conditions outside of disturbed zone, even at 1000 years.

**Case2: High Permeability Carbonates.** Whereas Case 1 specified uniform permeabilities, on the order of the absolute lowest feasible tuff permeability in the domain, the second case increases the permeability in the carbonates to  $1 \times 10^{-14} \text{ m}^2$ , consistent with the estimates of Winnograd and others (1975) (see Table 3). All other parameters remain the same as those used in Case 1. Adding the higher permeability to the carbonate unit does not have an impact on the distribution of hydraulic head in for the observations in the volcanic tuff at the elevation of the test. But it does increase the dissipation of head in the carbonates. Figure 13 shows the head response over the domain during the first hundred years for this case. Figure 14 shows the time histories for the line 3 observation points. They are virtually identical to those in Figure 11. The only difference was seen on observation line 1 (Fig. 15) where there are nodes actually located in the carbonate aquifer. Including two observations,  $1.82r$  and  $1.53r$  which are within the  $2r$  domain. The higher permeability in the carbonate aquifer aids in the rapid dissipation of hydraulic head in that particular area.

**Case 3: Accounting for Non-Zeolitic Tuff and Carbonate Aquifer.** The tuffs in Yucca Flat are not completely homogenous. Not only is there variation between the different units, but material properties are expected to vary with secondary alteration (zeolitization) as well. Tuff permeability data from Yucca Mountain (Flint, 1998) indicate a significant difference between zeolitic and non-zeolitic tuffs within the same HSU. Therefore, this case examines the effect of higher permeability (from the Case 1) in unaltered tuff.. For this simulation, the permeabilities in non-zeolitized units range from  $1\text{-}3 \times 10^{-15} \text{ m}^2$ , and the zeolitized permeabilities are held in the range of  $1\text{-}3 \times 10^{-19} \text{ m}^2$ . The carbonate permeability is set at  $1 \times 10^{-14} \text{ m}^2$ , as in Case 2. There are two subsets of Case 3 that are considered, differing from each other in how the porosity in the disturbed zone is specified. In the first subset, the porosities for each unit, in and away from the disturbed zone remain as prescribed in Table 4. In the second subset, the porosities in the disturbed zone are reduced an order of magnitude from the undisturbed values.

**Subset Case3a: No Porosity Reduction in the Disturbed Zone.** Figure 16 and Figure 17 show that the hydraulic head perturbation in the disturbed zone dissipates rapidly at all observation points in this simulation. The hydraulic heads have returned to pre-testing conditions within the first year of the simulation. The mixture of high permeability non-zeolitic tuff and low permeability zeolitic tuff are effective in dissipating the pressure pulse. This is primarily due to some unique features about the particular test examined in the study, and probably do not pertain to all of the other tests. As indicated in Table 3 all of the observation points outside of the cavity are either in the carbonate or the unaltered tuff. Because the permeability in the cavity is specified to be high, all of the observation points along lines 1 and 3 are in a connected high permeability pathway which dissipates pressure rapidly. Although not shown in these figures, observation points in the zeolitized tuff sustain the pressure perturbation much longer, similar to the results in Case 1.

**Subset Case3b: Porosity Reduced in the Disturbed Zone.** This case is identical to Case 3a, except the porosity is reduced to 0.05 in the disturbed zone. Figure 18 shows the observations on line 3 and Figure 19 shows the response along line 1 for this case. Figure 20 shows the head response over the domain during the first hundred years for this case. What is particularly surprising about this figure is that the head returns to ambient conditions almost immediately everywhere in the domain. Based on the results from Case 1, we would have expected the

pressure to remain high in the low permeability zeolitic units for a long time. But, somehow there is enough hydraulic connection with the high permeability tuffs and carbonates to dissipate the pressure anomaly rapidly at all locations in the domain. The reduction in porosity in the disturbed zone leads to less high pressure water available for dissipation. Therefore, the response at observation points is smaller for this case than it was in Case 3a.

**Case 4: Specifying low permeability in disturbed zone.** The previous cases have not considered specific permeability changes in the disturbed zone. Whereas Case 1 shows that if the background permeabilities are low enough, the pressure pulse is sustained for a long time, Case 3 shows that with higher permeabilities (in the unaltered tuff and carbonates) the pressure pulse dissipates quickly if there is a connected high permeability pathway. Case 4 looks at the effects of permeability and porosity changes in the disturbed zone, even when higher permeability tuffs and carbonate rocks are present in the formations in which the tests are conducted (or the cavities extend). This case assumes that compressional shock waves reduce the permeability in the disturbed zone (to  $1 \times 10^{-19} \text{ m}^2$  for evaluation purposes). Two subsets examine the cases for unaffected and reduced porosity in the disturbed zone. Thus this case extends the two subsets in Case 3 in which carbonates and unaltered tuff have relatively high permeability and zeolitized tuff has low permeability. The extension is the reduction of permeability in the disturbed zone, regardless of whether the host tuff was altered or not.

**Subset Case 4a: No reduction in porosity.** Figures 21 and 22 show that reducing the permeability in the disturbed zone leads to slow dissipation of the pressure perturbation. Outside of the disturbed zone, at observation points in either the high permeability carbonates (e.g. 2.1r in line 1) or the high permeability unaltered tuff (all points beyond 2r in line 3), the pressure wave dissipates rapidly, just as in Case 3. Thus, under these conditions, the sustained water mound is only predicted to remain in the disturbed zone where the permeability is sufficiently low. However, an extension of this evaluation would be to simply look at the pressure response in the zeolitized tuff outside of the disturbed zone. We anticipate that the response would be similar to that at points outside the disturbed zone in Case 1, where the permeability is set low for zeolitized tuff everywhere.

**Subset Case 4b: Porosity reduced in disturbed zone.** This case is identical to 4a with the exception that the porosity is reduced in the disturbed zone. Figure 23 shows the domain response to the pressure anomaly for this case. As in Case 1, the low permeability in the disturbed zone for Case 4 serves to maintain the high pressure for longer time than Cases 2 and 3. Although the differences are minor, the change in porosity in the disturbed zone increases the rate of dissipation of head perturbation. However, Figures 24 and 25 show that this slight increase in dissipation does not result in an appreciable ground water mound in the high permeability carbonates that is sustainable beyond the first year of the simulation.

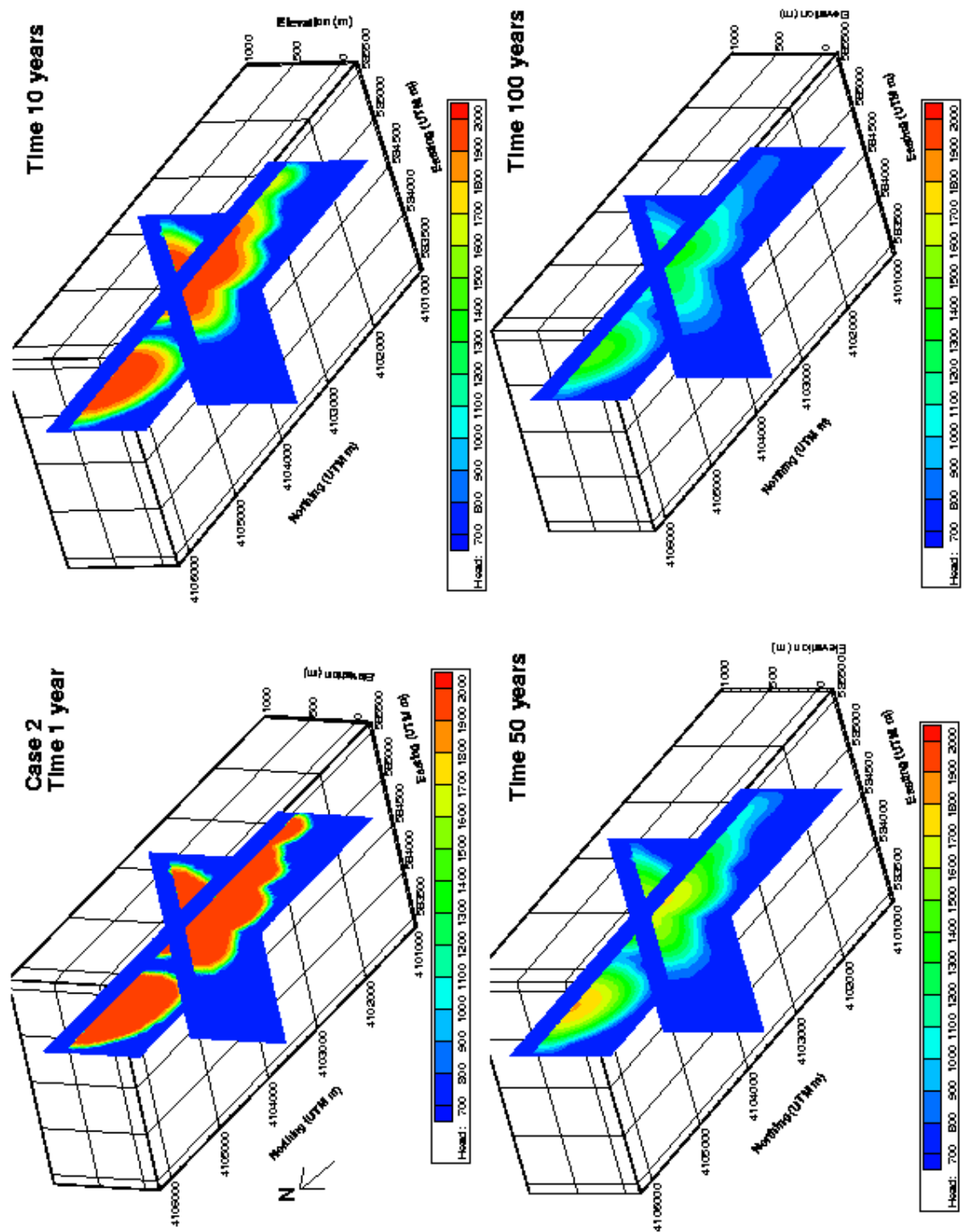
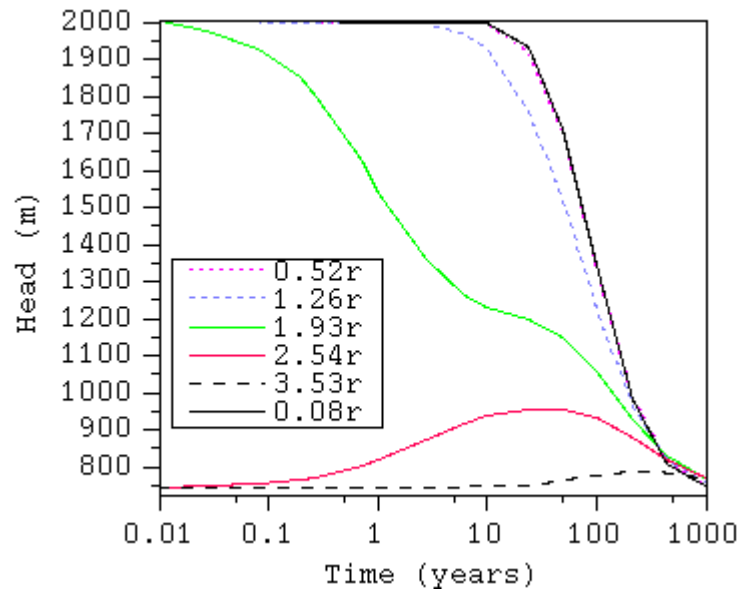
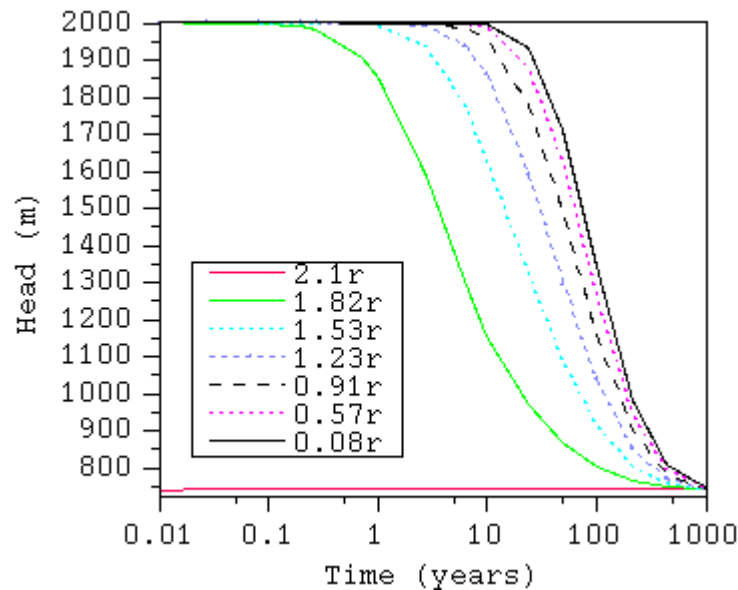


Figure 13. Head response throughout domain over first 100 years for Case 2 conditions.



**Figure 14.** Simulated head responses on observation line 3 for Case 2. Head responses are virtually identical to Case 1 (c.f.), demonstrating that the dissipation of hydraulic head in the upper tuff units is unaffected by the addition of the high perm carbonate aquifer properties.



**Figure 15.** Simulated head responses on observation line 1 (downward from working point) for Case 2. Clearly the head pulse dissipates rapidly in the high permeability carbonate aquifer, leading to no perceptible response at observation point 2.1r (in carbonates). Comparison with Figure 12 shows some increased dissipation of the initial pulse within the disturbed zone (up to 2r). The increase dissipation is the result of observations at 1.82r and 1.53r which are also in the high permeability carbonate aquifer.

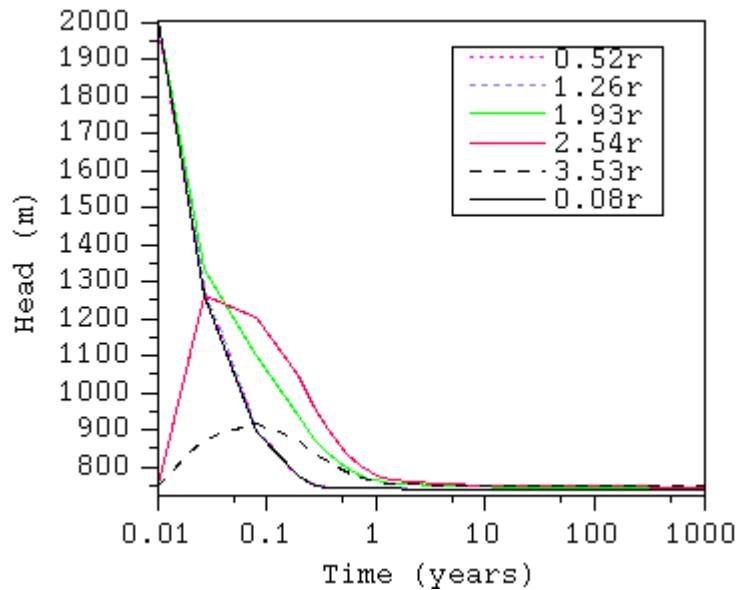


**Figure 16.** Simulated head responses on line 3 for Case 3a. Outside of the cavity, all observation points are in unaltered, high permeability tuff. The connected pathway of high permeability material from the cavity to the boundary allows rapid dissipation of pressure.

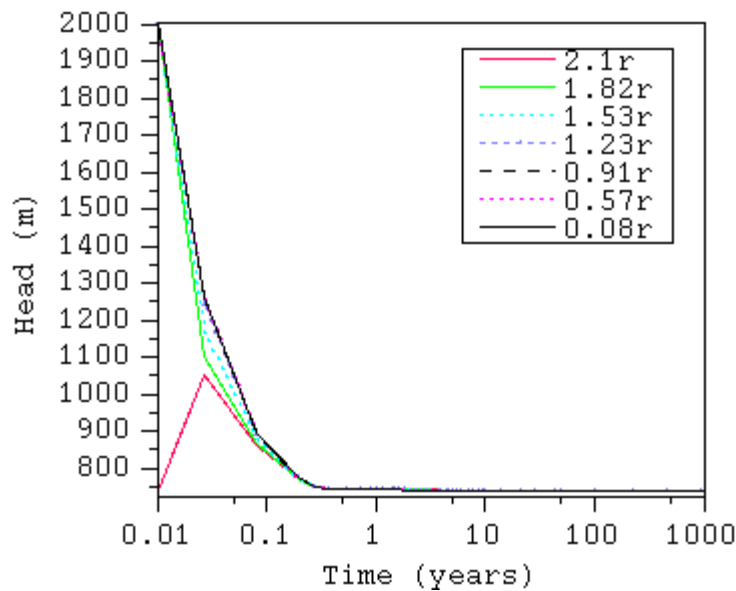


**Figure 17.** Simulated head responses on line 1 for Case 3a. Outside of the cavity, all observation points are in high permeability carbonates. As pressure dissipates quickly on the connected pathway of high permeability material from the cavity to the carbonate aquifer, a sudden spike in hydraulic head moves through the observation point at 2.1r in the carbonate aquifer.

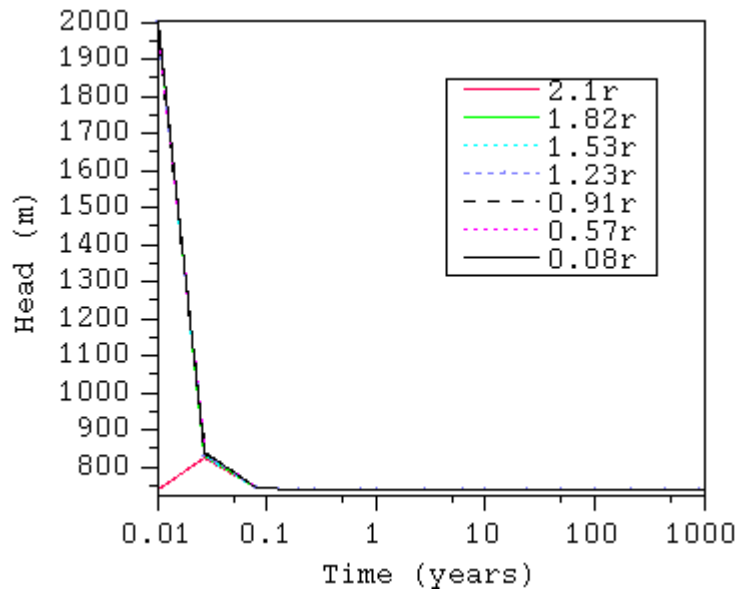


**Figure 18.** Simulated head responses on line 3 for Case 3b. Outside of the cavity, all observation points are in unaltered, high permeability tuff. The connected pathway of high permeability material from the cavity to the boundary allows rapid dissipation of pressure. As compared to Figure 10, the reduction of porosity in the disturbed zone leads to smaller peaks outside of the disturbed zone and the time required for the increased head to dissipate in all areas was decreased, both due to decreased storage resulting from lower porosity.

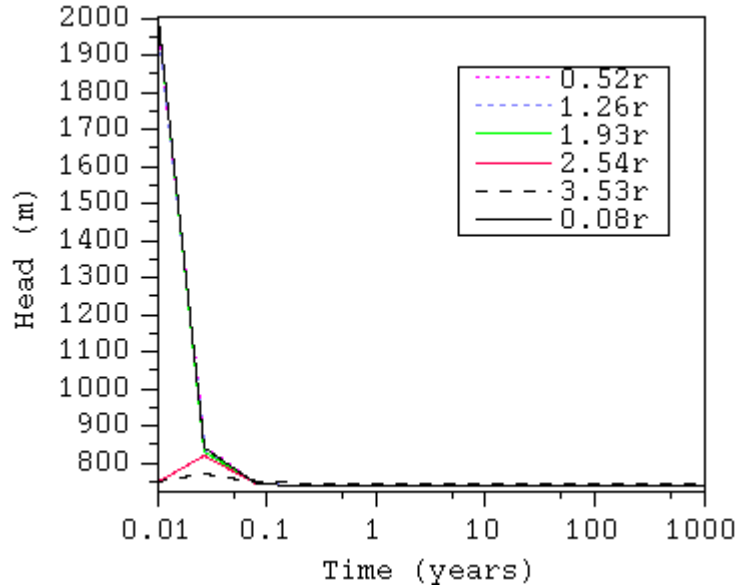


**Figure 19.** Simulated head responses on line 1 for Case 3b. Outside of the cavity, all observation points are in high permeability carbonates. As pressure dissipates quickly on the connected pathway of high permeability material from the cavity to the carbonate aquifer, a sudden spike in hydraulic head moves through the observation point at 2.1r in the carbonate aquifer. Compared with Case 3a, the peak in the carbonates at early time is smaller due to reduced porosity (and storage) in the disturbed zone.

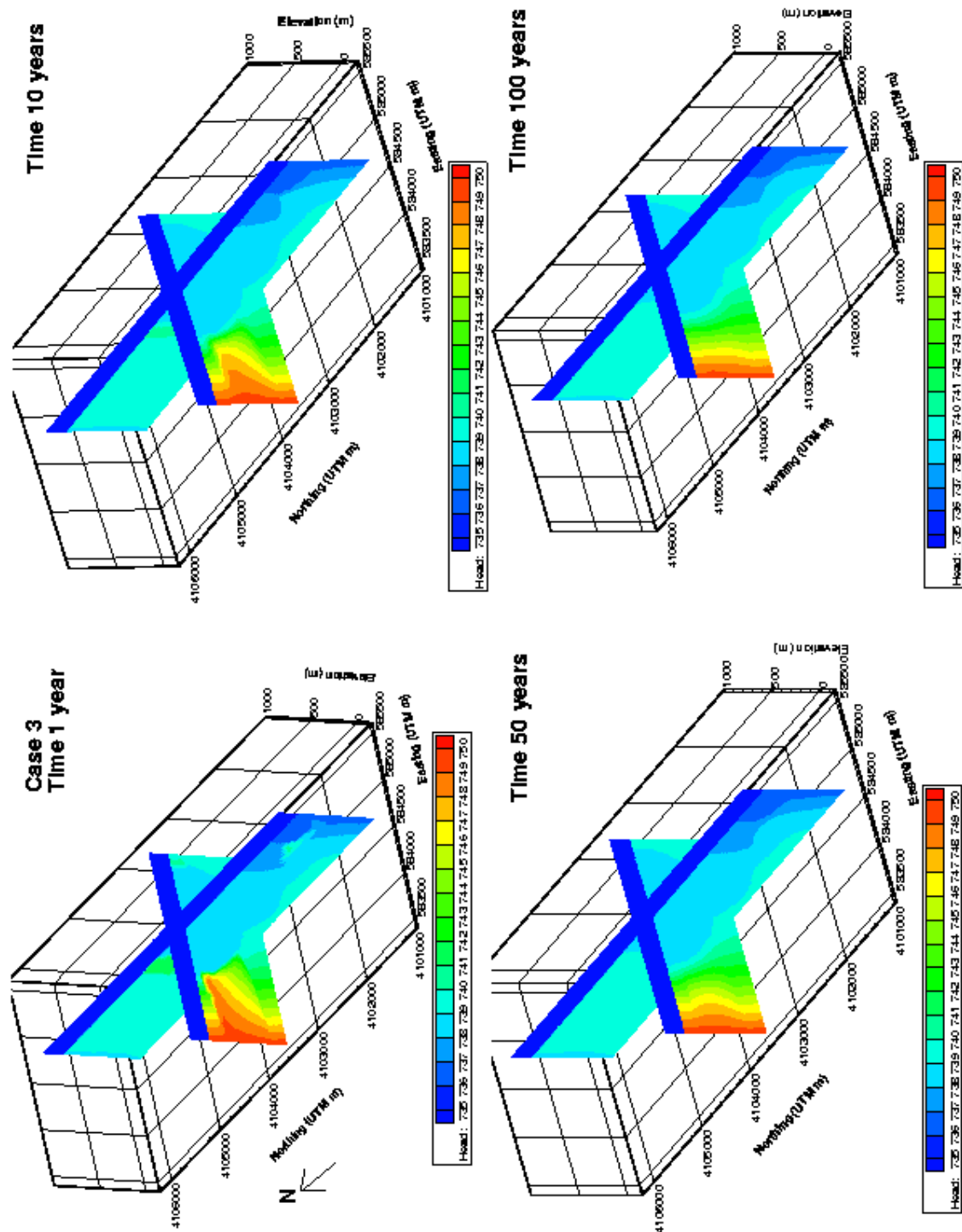
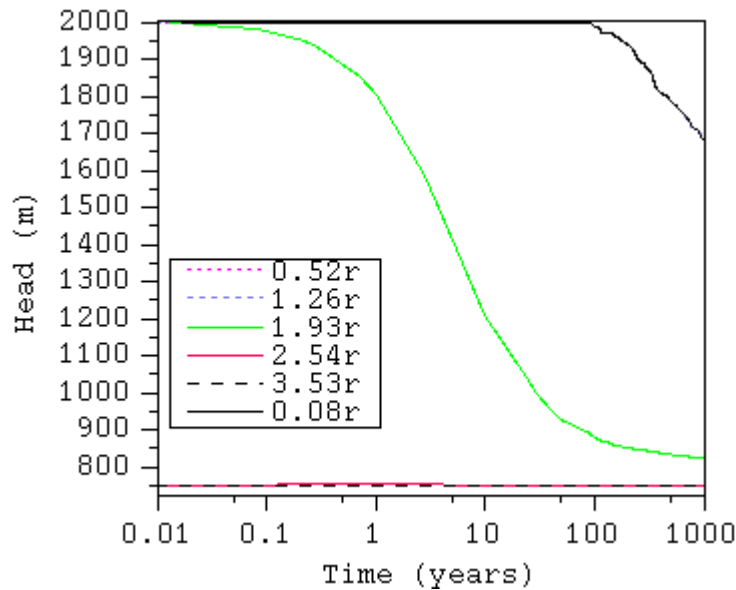
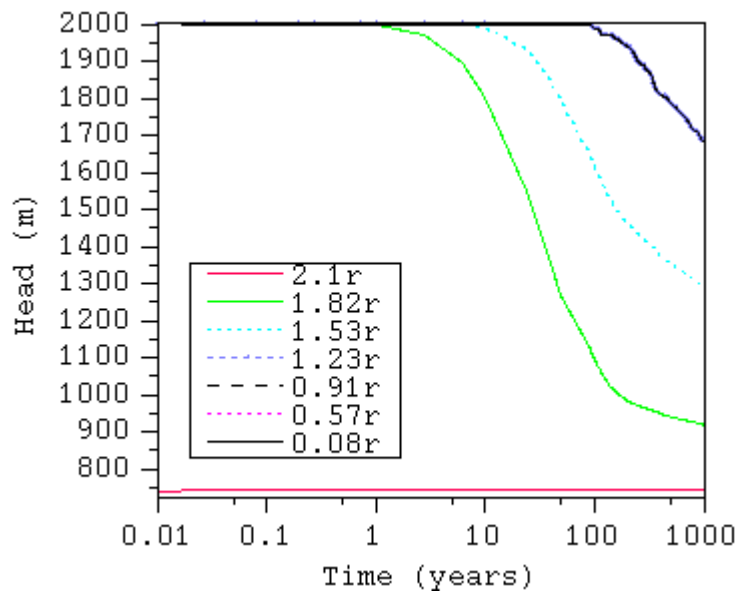


Figure 20. Head response throughout domain over the first 100 years for case3b conditions.



**Figure 21.** Simulated head response along line 3 for Case4a. The dissipation of the hydraulic head perturbation is immediately damped in the high flow, high permeability unaltered tuff zone outside of the disturbed zone.



**Figure 22.** Simulated head response along line 1 for Case4a. The dissipation of the hydraulic head perturbation is immediately damped in the high flow, high permeability carbonate zone below the disturbed zone ( $r > 1.5$ ).

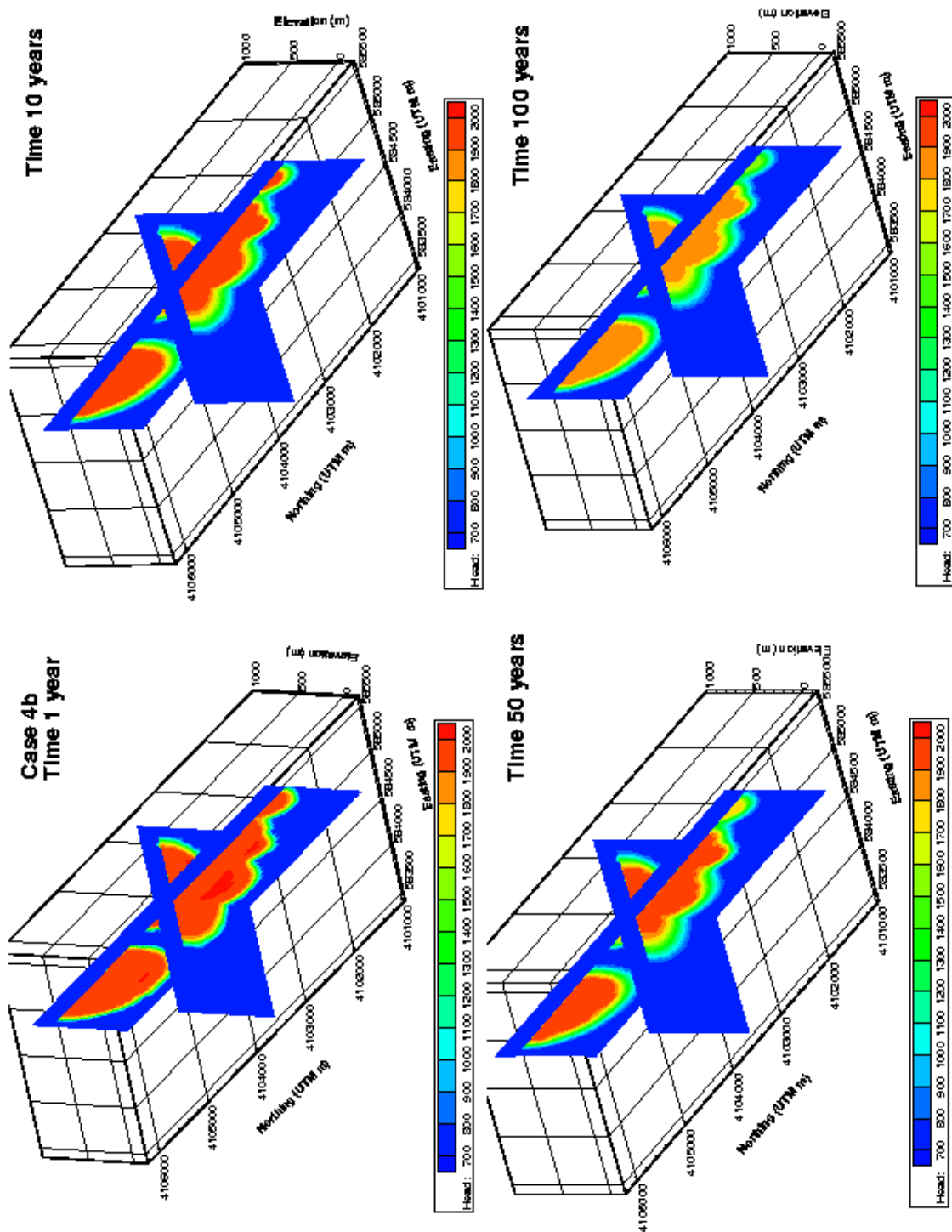


**Figure 23.** Head response for Case 4b. The low permeability disturbed zone serves to maintain the pressure anomaly for long time, similar to the zeolitic tuff in Case 1.

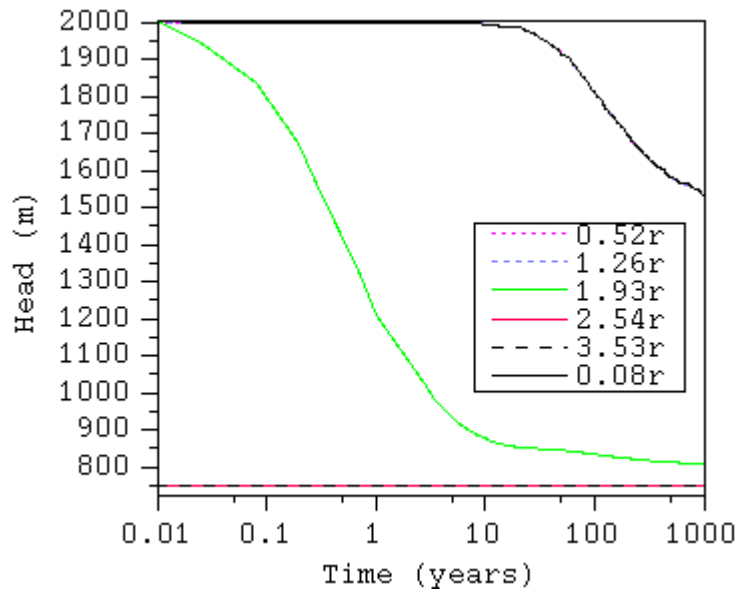


**Figure 24.** Simulated head response along line 3 for Case4b. Compared to Case4a, the reduced porosity leads to slightly faster dissipation of the hydraulic head perturbation within the disturbed zone due to reduction in storage there.

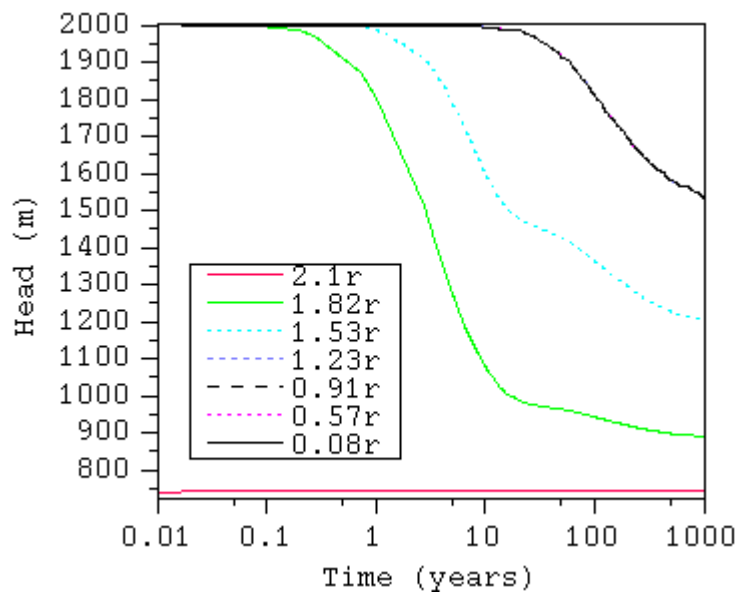


**Figure 25.** Simulated head response along line 1 for Case4b. As with line 3, the reduced porosity leads to slightly faster dissipation of the hydraulic head perturbation within the disturbed zone compared with Case4a due to reduction in storage.

## Summary of Test Results

The test cases described above examine the conditions and assumptions necessary to simulate a sustained ground water mound in and away from the disturbed zone of the Tuff Pile 1 in Yucca Flat. Although these are only scoping calculations, some preliminary assessments may be drawn from the results. It appears that low permeability is necessary for sustaining an elevated head response (a ground water mound) in and beyond the disturbed zone. High permeability tuffs and the carbonate aquifer dissipate any pressure anomalies rapidly. Therefore, in the absence of structural bounding features such as impermeable faults, it is unlikely that sustained mounding will be observed in high permeability units. It is also unlikely that faults or other structural features are capable of containing high pressure anomalies due to the multiple directions into which such high pressure could dissipate. Therefore, zones below the water table sustaining post-testing anomalies of elevated hydraulic head are most likely associated with low permeability material.

These simulations have examined head responses near and away from test-related perturbation for several different conditions. Although simple in parameter distribution, Case 1 provides significant insight into pressure dissipation in low permeability zeolitized tuff. At locations far away from the working points (almost 4 cavity radii from Turquoise, a large test), elevated heads are simulated beyond 1000 years after testing. Due to the geometry of the observation points and the size of the Turquoise cavity (maximum estimated radius), Cases 2 and 3 ended up demonstrating how elevated pressure is not sustained when connected high permeability pathways are created between the cavity and the unaltered tuffs or the carbonate. Case 4, however, provides insight into the case where the permeability in the disturbed zone is reduced due to the underground explosion. Just like the low permeability zeolitic tuffs in Case 1, the reduced permeability disturbed zone sustains the pressure anomaly for long time.

## Transport

A preliminary evaluation of transport potential was examined for Case 3 since it represented the most likely conduit between shot #16 and the carbonate aquifer. In that case, the high permeability cavity is in direct contact with the high permeability carbonate aquifer. Two simulations were performed with the particle tracking module in FEHM. A swarm of particles were release first in the bottom of the cavity, to simulate release from the melt glass. Then a swarm of particles were released from the bottom of the disturbed zone, to consider the case that contaminants may have migrated to the extent of the disturbed zone at early time. Although only qualitative, Figure 23 shows the domain into which the particles migrated for the two cases. For particles starting inside the cavity, in the puddle glass region, virtually no migration outside of the cavity is simulated. For the case of particles starting on the outer edge of the disturbed zone, the initial pressure gradient between the disturbed zone and the carbonate aquifer drives them out into the carbonate aquifer. There, they migrate with the ambient flow toward the eastern boundary, as would be predicted by looking at the head contours in Figure 4. This transport scenario does not consider any sorption, decay, diffusion, or other transport mechanisms. It is more of a flow path mapping exercise. It is important to also note where the particles start in the two different cases and that for Case 3, there is no permeability reduction in the disturbed zone.

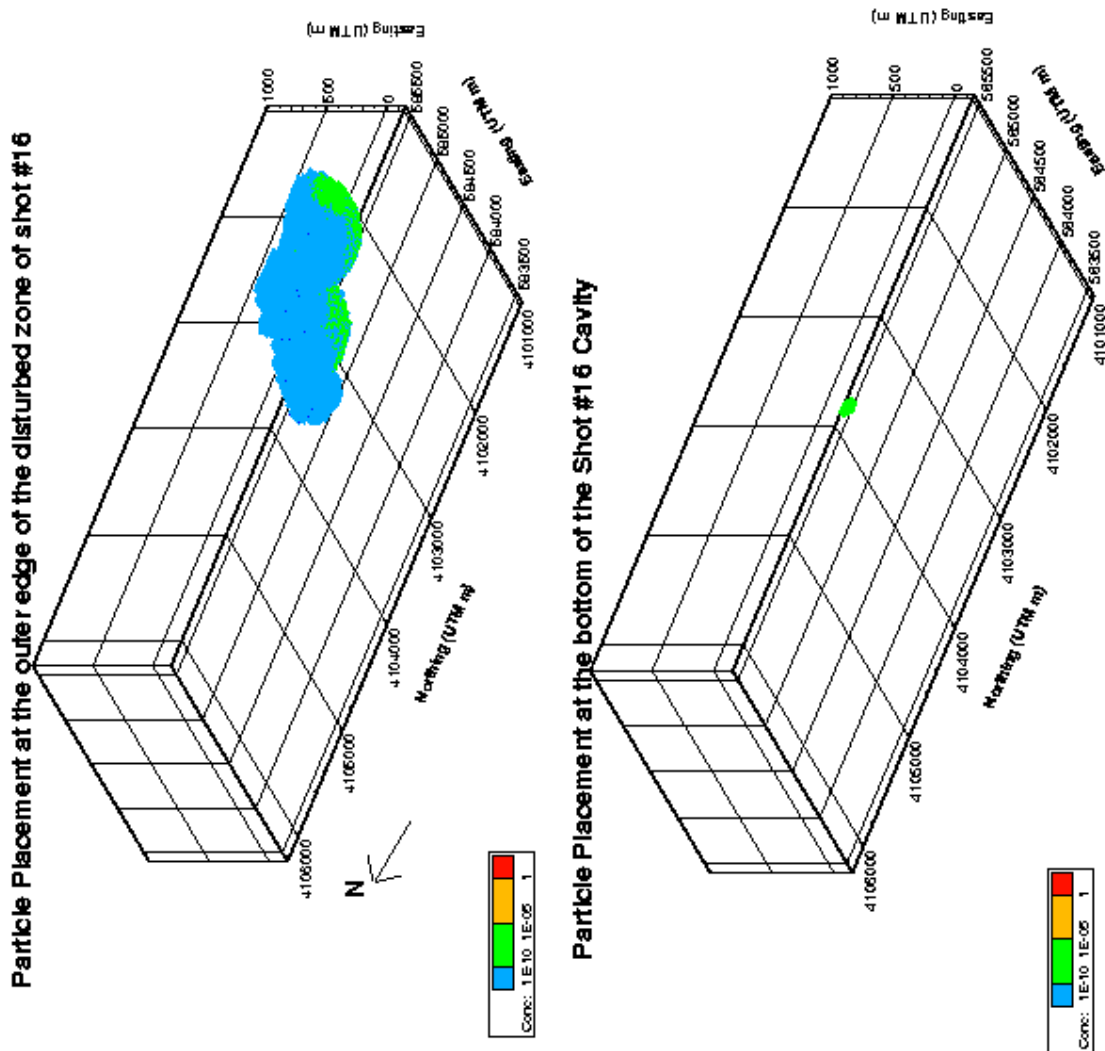


**Figure 26.** Particle transport simulations for Case 3b. Migration into the carbonates requires initiating particles at the edge of the disturbed zone, which is in the carbonates in this simulation. Particles starting in the cavity do not migrate, even with no retardation and decay considered.

## CONCLUSIONS AND FUTURE WORK

Scoping calculations show that if low permeability rocks surround underground nuclear tests, which initially pressurize the disturbed zone, an elevated hydraulic head mound may be created and sustained, even beyond the disturbed zone, for a substantial amount of time. For deeper tests, and particularly large tests, this zone of initially elevated hydraulic head may extend down into regional aquifer rocks. Also, such tests may create a high permeability conduit from the cavity to the regional aquifer, depending on the size of the cavity and the post-test permeability. It is possible that fluids originating near the external boundary of the disturbed zone, and maybe even from within the cavity, will eventually move into the regional aquifer. The existence of high permeability rocks, such as fractured welded tuffs or carbonate aquifer rocks within this zone of pressurization would cause the overpressure to dissipate rapidly if they are not altered significantly during the test.

We conclude that the simulation method is a viable tool for studying the problem of pressure response and contaminant migration from underground tests. While the hypothesis about the cause of observed water-mounding is still viable at this point in the study, the exact mode by which it arises has yet to be established. Whether water transport is required or not (Burkhard and Rambo, 1991) will depend upon more detailed simulations of the response of rocks within the disturbed zone around underground tests. Answering these questions will require looking at the cumulative effect of shots, establishing what is required to produce a ground water mound, and evaluating pre and post hydrogeologic properties surrounding a shot.

While App and Murasak (1997) have shown little variation in densities and porosities within individual stratigraphic units of the Tuff Pile 1, there are little if any measured permeabilities. Since permeability varies considerably depending upon the degree of fracturing and alteration (zeolitization), it is appropriate to determine a reasonable range for the Tuff Pile 1. The scoping simulations done here have shown that variations in permeability, both in and away from the disturbed zone, greatly effect the ability of the Tuff Pile 1 to sustain a water-mound.

To a large degree, this study is predicated by documentation of anomalous water levels monitored in emplacement and exploratory wells in the vicinity of Tuff Pile 1 (Wohletz and Hawkins, 1998). The measured water levels and their rate of rise above the expected static water level in these wells are a natural data set for our simulations. For example, at the Aleman (U3kz) emplacement hole, water level rose at a rate of 1.5 m/day to a level 64 m above the static water level. This information can be incorporated in further explorations of the Tuff Pile 1 with a time series analysis of shot effects.. Namely, whereas this study involved the model development and preliminary scoping calculations, the logical next step is to include a shot-by-shot analysis on the cumulative effect throughout the domain, focussing on locations of anomalous observations.

Transport modeling of solute migration will involve three-dimensional transport simulations using the techniques that have been developed for the Pahute Mesa transport studies. Namely, issues of colloid transport, fracture-matrix interactions, and groundwater chemistry will be considered.

An obvious extension of this set of simulations would include looking at locations further north in the three-dimensional model than were examined here. Examining the response in and away from disturbed zones that did not extend all the way down to the carbonates and all the way into the unaltered tuff will demonstrate the far field effects of, perhaps, more representative testing in the Tuff Pile. The current model is capable of such additional simulations.

## REFERENCES

- App, F. N. and Marusak, N. L., 1997, Tuff Pile 1 - a justification for the projection of material properties within a portion of Los Alamos Test Areas 1, 3, 4, and 7 - Nevada Test Site. Los Alamos National Laboratory report LA-UR-97-1024, Los Alamos, NM, 45 p.
- Burkhard, N. R. and Rambo, J. T., 1991, One plausible explanation for water mounding: Proceedings of the Sixth Symposium on Containment of Underground Nuclear Explosions. Lawrence Livermore National Laboratory CONF-91 2, 145-158.
- Drellack, S. L., Jr., 1994, UGTA cross sections through southern Yucca Flat, Ratheon Services Nevada, File No. 7100.2, Corres. No. TSP:DGP:027:95.
- Flint, L.E. 1998. Characterization of Hydrogeologic units using matrix properties, Yucca Mountain, Nevada, USGS WRI Report 97-4243.
- Hawkins, W. L. and Cavazos, A. P., 1987, Geologic and hydrologic investigations at the ALEMAN (U3kz) site, and other sites in Yucca Flat, the Nevada Test Site. In: Proceedings of the Fourth Symposium on Containment of Underground Nuclear Explosions. Lawrence Livermore National Laboratory CONF-870961 2, 387-398.
- Hover, D. L. and D. A. Trudeau. 1987. High Fluid Levels in Drill Holes, Yucca Flat, Nevada Test Site. Proceedings of the Fourth Symposium on Containment of Underground Nuclear Explosions –Vol. 2. Edited by Olsen et. al. p.363-372.
- Laczniak, R.J. et. al. 1996. Summary of Hydrogeologic Controls on Ground-Water Flow at the Nevada Test Site, Nye County, Nevada. USGS WRI Report 96-4109.
- Winnograd, I.J and W. Thordarson. 1975, Hydrogeologic and Hydrochemical Framework, South-Central Great Basin, Nevada-California, with Special Reference to the Nevada Test Site. USGS Professional Paper 712-C.
- Wohletz, K. and Hawkins, W., 1998, Effects of Underground Nuclear Testing Below the Water Table on Groundwater and Radionuclide Migration in Areas 1, 3, 4, and 7 (*Tuff Pile I*), Yucca Flat, Nevada Test Site. EES-1 UGTA FY98 Report, Los Alamos National Laboratory, 22.

**Appendix A: Northwest Yucca Flat Underground Nuclear Tests**

Yr	Event	Easting (m)	Northing (m)	WP Elev (m)	H2O elev (m)	Yield* (kt)	Est. Cavity Radius (m)
64	Mackerel	584360.35	4105698.77	929.64	769.32	19.999	50
67	Zaza	584134.24	4106044.76	600.46	786.08	110	233
76	Billet	584996.56	4103457.61	613.26	762.31	85	182
77	Sandreef	584449.64	4103090.02	547.12	770.54	85	178
77	Crewline	584882.53	4105559.82	700.13	800.10	85	188
78	Transom	584199.47	4104826.08	618.44	782.73	0	0
78	Rummy	584324.46	4103942.81	613.26	779.38	85	182
78	Lowball	584995.58	4103823.58	687.63	766.88	85	188
79	Hearts	584185.32	4104863.21	618.75	788.52	138	296
80	Bonarda	584638.37	4101323.26	855.58	769.62	19.999	49
81	Trebbiano	584637.32	4101536.57	932.69	746.15	19.999	52
81	Baseball	584900.58	4104756.93	694.64	762.92	85	188
82	Jornada	584319.66	4105222.95	621.18	764.44	133.7	287
82	Bouschet	584857.32	4102756.25	680.62	771.15	85	188
82	Borrego	584883.70	4105224.32	697.69	766.57	149.999	332
83	Turquoise	584809.23	4103174.77	712.93	765.36	149.999	336
83	Coalora	584882.15	4101324.12	962.87	749.51	19.999	53
84	Vermejo	584186.75	4104543.25	905.26	786.08	19.999	50
84	Tortugas	584786.99	4102390.02	604.72	765.96	85	182
85	Vaughn	584881.40	4101537.42	812.60	752.55	85	202
86	Glencoe	583012.93	4104284.99	651.05	786.69	29	63
86	Aleman	584481.29	4102754.62	742.49	778.46	19.999	46
87	Tahoka	584880.28	4101857.69	601.07	767.79	19.999	43
88	Dalhart	584497.31	4104964.56	616.00	751.94	149.999	321
89	Tulia	583979.29	4104612.00	859.54	779.38	19.999	48
91	Lubbock	584879.01	4102131.94	782.42	745.24	85	198

\*From DOE/NV 209 (Rev. 14), 1994; midpoint if yield stated as range, maximum if stated as less than.